

## Performance-based structural fire design of steel frames using conventional computer software

Y.K. Chan<sup>1</sup>, C.K. Lu<sup>1</sup>, S.L. Chan<sup>2\*</sup> and F.G. Albermani<sup>3</sup>

<sup>1</sup>*Charterwealth Professional Ltd., Hong Kong*

<sup>2</sup>*The Hong Kong Polytechnic University, Hong Kong*

<sup>3</sup>*The University of Queensland, Australia*

*(Received December 29, 2008, Accepted April 1, 2010)*

**Abstract.** Fire incident in buildings is common, so the fire safety design of the framed structure is imperative, especially for the unprotected or partly protected bare steel frames. However, software for structural fire analysis is not widely available. As a result, the performance-based structural fire design is urged on the basis of using user-friendly and conventional nonlinear computer analysis programs so that engineers do not need to acquire new structural analysis software for structural fire analysis and design. The tool is desired to have the capacity of simulating the different fire scenarios and associated detrimental effects efficiently, which includes second-order P-D and P-d effects and material yielding. Also the nonlinear behaviour of large-scale structure becomes complicated when under fire, and thus its simulation relies on an efficient and effective numerical analysis to cope with intricate nonlinear effects due to fire. To this end, the present fire study utilizes a second-order elastic/plastic analysis software NIDA to predict structural behaviour of bare steel framed structures at elevated temperatures. This fire study considers thermal expansion and material degradation due to heating. Degradation of material strength with increasing temperature is included by a set of temperature-stress-strain curves according to BS5950 Part 8 mainly, which implicitly allows for creep deformation. This finite element stiffness formulation of beam-column elements is derived from the fifth-order PEP element which facilitates the computer modeling by one member per element. The Newton-Raphson method is used in the nonlinear solution procedure in order to trace the nonlinear equilibrium path at specified elevated temperatures. Several numerical and experimental verifications of framed structures are presented and compared against solutions in literature. The proposed method permits engineers to adopt the performance-based structural fire analysis and design using typical second-order nonlinear structural analysis software.

**Keywords:** fire analysis; finite element method; steel structures; nonlinear analysis

---

### 1. Introduction

In past decades or so, the fire safety design of the buildings was carried out to the fire design specifications, such as BS5950 Pt. 8 (2000) and Eurocode 3 Pt. 1.2 (1993), to assess the fire resistance of structural components under the international standardization for organization (ISO 834, 1985) for fire, which, for the time being, appears to suffer from a few limitations. For example, only an approximate and linearised structural behaviour can be predicted by the component check approach of the traditional fire safety design codes. In reality, the individual components exposed to fire are part of a

\* Corresponding author, Professor, E-mail: [ceslchan@polyu.edu.hk](mailto:ceslchan@polyu.edu.hk)

large structure, and much of the members remain cool during fire. The intact part of the structure may support and restraint the weakened components due to heating. To design a structure safely and economically, the complete structure should be therefore considered as an entity instead of a collection of isolated components which are designed individually. Computer software for fire analysis can be used for the fire safety design of a complete structure allowing for different thermal effects and associated nonlinear structural effects. In addition, the fire safety design of the large-scale building structures is urgently required in pace with the simulation-based approach in the future. The performance-based fire safety design approach is worthy of further research and development, which attributes to cost saving, enhanced safety level and efficient design. In most cases, the interaction effects among the heated and cool members on the complete structural system under fire scenarios are complicated and tedious by means of manual calculation using the prescriptive fire safety design. Thus, the advanced numerical fire analysis for the future fire safety design is imperative and proposed in this paper using typical second-order analysis software. Jeanes (1982, 1985) presented the fire analysis including two-dimensional element for simulating the floor system under fire. In this study, members in the frame are modeled by the beam-column elements and the non-conforming triangular plate bending element is used to model the floor slab. However, this analysis requires great computational effort and thus it may not be suitable for the fire safety design of a large-scale building structure.

In continental Europe, researchers including Dotreppa *et al.* (1982) and the ARBED Research Center (1982, 1992) studied the structural behaviour of beams, columns and frames under fire by the finite element method. Schleich *et al.* (1986) developed the nonlinear fire analysis using the incremental-iterative Newton-Raphson solution procedure to cope with the nonlinearities. Later Franssen (1987) presented a fire analysis which considers non-uniform temperature distribution, material yielding and geometric nonlinearities. Franssen (1990) modified the constitutive law including loading-unloading response and developed the user-friendly computer program SAFIR (Franssen *et al.* 2000) using a fine grid of elements over each cross-section. Based on the computer program SAFIR, Lim *et al.* (2004a, b) investigated the fire behaviour of two-dimensional reinforced concrete slab under fire. Vila Real *et al.* (2004) presented a comparative study between numerical results by SAFIR (2000) and fire design code - Eurocode 3 (1993).

In the United Kingdom, Saab and Nethercot (1991) presented the nonlinear structural behaviour of a plane frame subject to fire by the finite element method. Their basic numerical formulation of the nonlinear solution at ambient condition was mainly based on the research work from El-Zanaty and Murray (1983) on which Najjar and Burgess (1996) further utilized their previous works to develop the fire analysis software VULCAN. Similarly, Bailey (1998) based on this work to separately develop the computer program 3DFIRE. This basic nonlinear formulation allows the modeling of semi-rigid connections, lateral-torsional buckling, continuous floor slabs and strain reversal. Huang *et al.* (1999) extended their previous work further to incorporate the two-dimensional finite element in their fire analysis in order to model the behaviour of reinforced concrete slabs under fire. Later Huang *et al.* (2000) carried out a nonlinear three-dimensional fire analysis using VULCAN for composite framed structure using the finite element procedure.

Liew *et al.* (1998) presented the performance-based and nonlinear fire analysis of the steel framed structures. Material yielding behaviour is considered by plastic hinges formed at the element ends and the mid-span. The member is then divided into two elements when a plastic hinge is formed at the mid-span. Recently, Ma and Liew (2004) further developed their plastic hinge approach on their fire analysis to study three-dimensional bare steel frames under fire. In the paper, Liew (2004) provides an overall view on performance-based code and the approaches for designing steel structures in fire considering a multi-dimensional integration of fire simulation, heat transfer analysis, emergency evacuation

and structural resistance. Various fire modes and heat transfer analysis methods are presented and basis to modeling of large deflection and plasticity using nonlinear analysis software is explained.

Iu and Chan (2004) presented a nonlinear fire analysis by the plastic hinge approach where all thermal effects are incorporated into the stiffness formulation of the cubic finite element. Later, Iu *et al.* (2005) extended the fire analysis to consider the structural effects in the cooling phase in which the plastic strains are formulated in the stiffness formulation to account for permanent deformations during cooling. The plastic hinge method on the fire analysis was refined by Iu *et al.* (2007) to allow for the axial residual strength of the member after yielding, which is important to model the catenary action when a beam experiences significant large deflection.

Simulation-based nonlinear fire analysis is an important development of the fire safety design for the framed structures, especially for the large-scale steel structures because of its complexity under fire. To this end, this paper presents a fire study of the bare steel frames using structural analysis software NIDA (2007) to tackle the nonlinear behaviour of the framed structures exposed to fire. Its numerical stiffness formulation is derived from the fifth-order displacement function, namely the PEP element 1995, which can simultaneously satisfy both equilibrium and compatibility conditions at midspan of an element. The solution of nonlinearities is resorted to the incremental-iterative solution procedure, such as the Newton-Raphson method. Based on a set of temperature-stress-strain curves to BS5950 Part 8 (2000), material degradation due to rising temperature is taken into consideration by using the equivalent section properties. The thermal expansion is also incorporated in the thermal analysis of NIDA (2007). In dealing with the effect of material nonlinearity, the secant elastic modulus at the various temperatures is directly used in the analysis software NIDA (2007). This complete analysis procedure can be carried out in any nonlinear structural analysis software without modifying the source code, which implies that engineers can do the same for his structures using his familiar non-linear structural analysis software.

## 2. Basic numerical formulation of PEP element

According to the finite element approach, the basic stiffness formulation in the present analysis is based on the fifth-order displacement function to form the self-equilibrium element namely as the PEP element 1995 (Point-wise equilibrium polynomial). The main feature of this PEP element is to consider the member bowing effect implicitly in the element stiffness formulation, so a single element can be used to predict the flexural buckling behaviour of a member.

The second-order effects due to member bowing and flexural bending are introduced in the internal strain energy expression in Eq. (1) by inclusion of second-order terms. The total potential energy for nonlinear analysis of beam-column element under normal temperature can therefore be written as

$$U = \frac{EA}{2} \int_{-L/2}^{L/2} \left( \frac{du}{dx} \right)^2 dx + \frac{EI_z}{2} \int_{-L/2}^{L/2} \left( \frac{d^2v}{dx^2} \right)^2 dx + \frac{P}{2} \int_{-L/2}^{L/2} \left( \frac{dv}{dx} \right)^2 dx + \frac{EI_y}{2} \int_{-L/2}^{L/2} \left( \frac{d^2w}{dx^2} \right)^2 dx + \frac{P}{2} \int_{-L/2}^{L/2} \left( \frac{dw}{dx} \right)^2 dx \quad (1)$$

The external work done,  $V$  is equal to the applied force multiplied by the corresponding displacement as follows

$$V = \{d\}^T \{f\} \quad (2)$$

in which  $u$ ,  $v$  and  $w$  are the axial deformation and lateral displacements in the direction in  $y$ -axis and  $z$ -axis, respectively.  $EA$  and  $EI$  are the axial rigidity and flexural rigidity about corresponding axes, respectively.  $P$  is the axial member load. And  $\{d\}$  and  $\{f\}$  are the column vectors of the displacement and external applied force with respect to the corresponding degrees of freedom.  $\{d\}$  is a displacement column vector given by  $\langle u_1, u_2, v_1, v_2, w_1, w_2, \theta_{1x}, \theta_{2x}, \theta_{1z}, \theta_{2z}, \theta_{1y}, \theta_{2y} \rangle^T$ .

The total potential energy functional can be expressed as the sum of the strain energy and the external work done as,

$$\begin{aligned} \Pi &= U - V \\ \Pi &= \frac{EA}{2} \int_{-L/2}^{L/2} \left( \frac{du}{dx} \right)^2 dx + \frac{EI_z}{2} \int_{-L/2}^{L/2} \left( \frac{d^2v}{dx^2} \right)^2 dx + \frac{P}{2} \int_{-L/2}^{L/2} \left( \frac{dv}{dx} \right)^2 dx + \frac{EI_y}{2} \int_{-L/2}^{L/2} \left( \frac{d^2w}{dx^2} \right)^2 dx + \frac{P}{2} \int_{-L/2}^{L/2} \left( \frac{dw}{dx} \right)^2 dx - \{d\}^T \{f\} \end{aligned} \quad (3)$$

By the principle of stationary total potential energy, the equilibrium condition and thus the stiffness coefficients can be obtained by taking the first variation of the functional as

$$\delta\Pi = \frac{\partial\Pi}{\partial u_i} + \frac{\partial\Pi}{\partial q} \frac{\partial q}{\partial u_i} = 0 \quad \text{For } i = 1, 2, 3 \quad (4)$$

The element matrix in three-dimensional space can be extended directly from the foregoing equations by considering the stiffness in the  $y$ - and  $z$ -axes as

$$M_{1n} = \left[ \frac{EI}{L} \right]_n [c_{1n}(\theta_{1n} + \theta_{2n}) + c_{2n}(\theta_{1n} - \theta_{2n})] \quad (5)$$

$$M_{2n} = \left[ \frac{EI}{L} \right]_n [c_{1n}(\theta_{1n} + \theta_{2n}) - c_{2n}(\theta_{1n} - \theta_{2n})] \quad (6)$$

$$P = EA \left[ \frac{e}{L} + \sum_{n=y,z} (b_{1n}(\theta_{1n} + \theta_{2n})^2 + b_{2n}(\theta_{1n} - \theta_{2n})^2) \right] \quad (7)$$

$$M_t = \frac{GJ + Pr^2}{L} \theta_t \quad (8)$$

in which  $GJ$  is torsional rigidity.  $M_t$  is torsional moment.  $\theta_t$  is twist angle.  $r$  is polar radius of gyration. And  $n = y, z$ - principal axes. The numeric subscript stands for node number.  $c_{1n}$ ,  $c_{2n}$ ,  $b_{1n}$  and  $b_{2n}$  are the incremental secant stiffness coefficient, which are given by Chan and Zhou (1995).  $e$  is axial deformation.  $\theta$  is the element nodal rotations.

The tangent stiffness matrix relates the incremental change in forces to a corresponding change in displacements. This can be obtained by taking the first variation of the secant stiffness matrix with respect to the displacements at the degrees of freedom as

$$\delta^2 \Pi = \frac{\partial^2 \Pi}{\partial u_i \partial u_j} \delta u_i \delta u_j = \left[ \frac{\partial(\delta \Pi)}{\partial u_j} + \frac{\partial(\delta \Pi)}{\partial q} \frac{\partial q}{\partial u_j} \right] \delta u_i \delta u_j \quad (9)$$

The tangent stiffness matrix can finally be determined as

$$[K_T] = \sum^{Nele} [L][K_T][L]^T = \sum^{Nele} [L]([T]^T[K_e][T] + [N])(L)^T \quad (10)$$

in which  $[T]$  is transformation matrix relating the member basic forces to the element force in the local coordinate.  $[L]$  is local to global transformation matrix. And  $[N]$  is a matrix to account for the stiffness change due to the initial force and the translational displacements.

### 3. Nonlinear solution procedures

A nonlinear incremental-iterative procedure is used in this study to trace the nonlinear equilibrium path due to the geometric nonlinearities i.e. the P- $\Delta$  and P- $\delta$  effects. An incremental-iterative solution procedure is developed to cope with either the constant load increment of Newton-Raphson method or varied load increment, such as the arc-length method by Crisfield 1981 or the minimum residual displacement method by Chan 1988. The solution procedure of constant load Newton-Raphson method is schematically shown in Fig. 1 at temperature  $T^oC$ , which is basically used in the present approach.

Based on Newton-Raphson method to formulate the nonlinear solution procedures, the simple compact matrix form of equilibrium equation at a particular  $t$ -th temperature level ( $T^oC$ ) can be expressed as

$$\{f\} - [K_s]\{u\} = [K_T]\{\Delta u\} \quad (11)$$

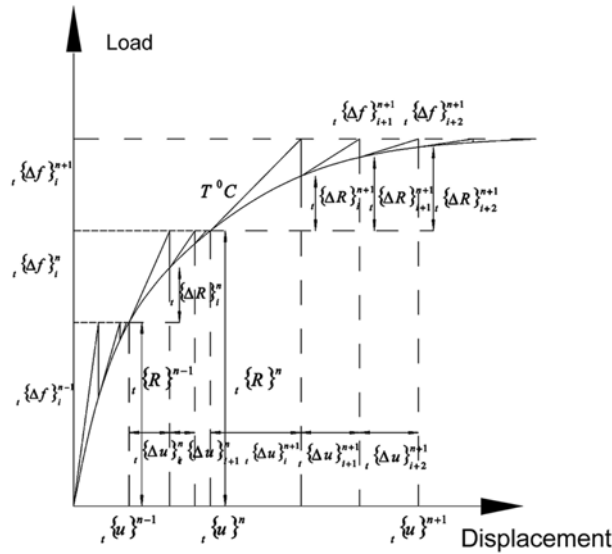


Fig. 1 Incremental-iterative scheme of Newton-Raphson method at t-th thermal cycle

in which  $[K_s]$  is secant stiffness which represents the internal member resistances. And  $\{f\}$  is applied loading.

In the constant load Newton Raphson scheme, the incremental displacement can be determined by the tangent stiffness in Eq. (12), and the total displacement is obtained by accumulation of incremental displacements in Eq. (13). In the meantime, the structural geometry is revised according to the updated Lagrangian formulation.

$${}_i\{\Delta u\}_{i+1}^n = [{}_iK_T(\{R\}_i^n)]^{-1} {}_i\{\Delta f\}_i^n \quad (12)$$

$${}_i\{u\}_{i+1}^n = {}_i\{u\}_i^n + {}_i\{\Delta u\}_{i+1}^n \quad (13)$$

in which  $[_iK_T(\{R\}_i^n)]$  is the incremental tangent stiffness at  $\{R\}_i^n$ .  ${}_i\{\Delta f\}_i^n$  is the unbalanced force between external applied load and internal member resistance. The incremental displacements in global coordinates can be transformed to the member deformations  ${}_i\{\Delta u\}_{i+1}^n$  by multiplying the transformation matrix  $[L]^T$ .  ${}_i\{\Delta R_e\}_{i+1}^{n+1}$  can then be evaluated in local coordinates as,

$${}_i\{\Delta u_e\}_{i+1}^n = [L]^T {}_i\{\Delta u\}_{i+1}^n \quad (14)$$

$${}_i\{\Delta R_e\}_{i+1}^n = [K_s({}_i\{R\}_i^n)] {}_i\{\Delta u_e\}_{i+1}^n \quad (15)$$

in which  $[K_s({}_i\{R\}_i^n)]$  is the incremental secant stiffness at  ${}_i\{R\}_i^n$ . After determination of the member resistant forces, the incremental member resistance is accumulated to the total member resistance in global coordinates as,

$${}_i\{R\}_{i+1}^n = {}_i\{R\}_i^n + [T][L] {}_i\{\Delta R_e\}_{i+1}^n \quad (16)$$

in which  $[T]$  is the transformation matrix from member coordinate to global coordinate. The unbalanced force  ${}_i\{\Delta f\}_{i+1}^n$  is therefore obtained as,

$${}_i\{\Delta f\}_{i+1}^n = {}_i\{f\}^n - {}_i\{R\}_{i+1}^n \quad (17)$$

The above incremental-iterative procedure is repeated for a specified temperature level ( $T^\circ C$ ) until equilibrium point is achieved at specified applied load level. The applied load is kept constant throughout the heating sequence. The next thermal cycle ( $(T+I)^\circ C$ ) starts with the same incremental-iterative procedure, when the constant load Newton-Raphson method is utilized as Eqs. (11)-(17), which is graphically shown in Fig. 2. The process is repeated throughout the thermal history until a numerical divergence is detected.

#### 4. Thermal analysis of PEP element

The thermal effects considered in the present fire analysis, mainly consist of thermal expansion and material degradation due to heating, where the thermal creep effect is only implicitly considered by a set of temperature-stress-strain curves. With respect to thermal expansion, once the temperature distribution across

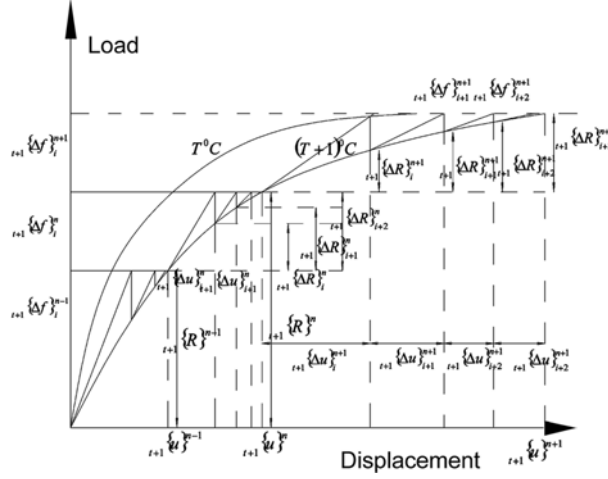


Fig. 2 Incremental-iterative scheme of Newton-Raphson method at (t+1)-th thermal cycle

the section has been determined, the change of the member length  $\Delta L$  resulting from rising temperature  $\Delta T$  can be evaluated as Eq. (18) based on the coefficient of thermal expansion coefficient  $\alpha$ , taken as  $12 \times 10^{-6}$ . The change of the member length can be converted to the nodal deformations  $\{\Delta u\}$  of a member in its axial directions. This deformed geometry of a structure due to rising temperature is treated as an initial geometry of the structure for subsequent second-order analysis. The change of geometry of the whole structural system can then be updated in accordance with the updated Lagrangian formulation in Eq. (19) as

$$\Delta L_i = \alpha \Delta T \times T \quad (18)$$

$${}_t\{u\}_0 = \{u\}_0 + {}_t\{\Delta u\} \quad (19)$$

The thermal effect on the physical properties of steel due to material degradation is considered in the reduction of the elastic modulus  $E_T$  and effective yield strength  $\sigma_{yT}$  in accordance with BS5950 Pt. 8 2000 and tabulated in Table 1. According to the present fire approach, material degradation is taken into

Table 1 Expressions of effective yield stress and elastic modulus for stress-strain- temperature curves

Temperature ( $^{\circ}C$ )	Yield stress, $\sigma_{yT} = \psi_T \sigma_{y20}$	Elastic modulus, $E_T = \psi_T E_{20}$
$80^{\circ}C < T \leq 400^{\circ}C$	$\sigma_{y20} \left( 0.978 - 0.034 \frac{T}{350} \right)$	$E_{20} \left[ 1 - 2.8 \left( \frac{T-20}{1485} \right)^2 \right]$
$400^{\circ}C < T \leq 550^{\circ}C$	$\sigma_{y20} \left( 1.553 - 0.155 \frac{T}{100} \right)$	$E_{20} \left[ 1 - 2.8 \left( \frac{T-20}{1485} \right)^2 \right]$
$550^{\circ}C < T \leq 600^{\circ}C$	$\sigma_{y20} \left( 2.34 - 0.22 \frac{T}{70} \right)$	$E_{20} \left[ 1 - 3 \left( \frac{T-20}{1463} \right)^2 \right]$
$600^{\circ}C < T \leq 690^{\circ}C$	$\sigma_{y20} \left( 1.374 - 0.078 \frac{T}{50} \right)$	$E_{20} \left[ 1 - 3 \left( \frac{T-20}{1463} \right)^2 \right]$
$690^{\circ}C < T \leq 800^{\circ}C$	$\sigma_{y20} \left( 1.12 - 0.128 \frac{T}{100} \right)$	$E_{20} \left[ 1 - 3 \left( \frac{T-20}{1463} \right)^2 \right]$

account through the equivalent deteriorated section properties, including area  $A_T$ , moment of inertia  $I_T$  and plastic section modulus  $Z_{pT}$ , to model the temperature variation effect in the physical properties of an element as (Landesmann *et al.* 2005).

The equivalent section properties of area  $A_T$  and moment of inertia  $I_T$  is evaluated from the stiffness deterioration (i.e.,  $E_T$ ) due to heating, whereas the equivalent plastic section modulus  $Z_{pT}$  is based on the strength deterioration (i.e.,  $\sigma_{yT}$ ) with increasing temperature. The finite element mesh across the steel section displayed in Fig. 3 is used to determine the equivalent section properties of a whole section, which depends on the temperature distributions on each segment. Based on this segmentation process, an equivalent cross section area  $A_T$  can be obtained by summation of the reduced area of each segment as Eq. (20), which is based on effective axial stiffness  $E_T A$  of the each segment shown in Fig. 3. To follow a similar methodology, an equivalent moment of inertia  $I_T$  can be obtained by Eq. (21) based on the effective bending stiffness  $E_T I$  of each segment. In this calculation, the reduction factor  $\psi_T$  of elastic modulus  $E_{20}$  in Table 1 is used to convert the section properties (i.e.,  $A$  and  $I$ ) at ambient condition into equivalent section properties (i.e.,  $A_T$  and  $I_T$ ) at elevated temperatures. It is interesting to note that the centroid of the section is assumed to remain unchanged against the temperature variation across the section. Also this methodology is only applicable to doubly symmetric steel sections.

$$E_{20}A_T = \int_A E_T dA = \int_A E_{20} \psi_T dA = E_{20} \sum_i^n \psi_{T,i} A_i$$

$$A_T = \sum_i^n \psi_{T,i} A_i \quad (20)$$

$$E_{20}I_T = \int_A E_T y^2 dA = \int_A E_{20} \psi_T y^2 dA = E_{20} \sum_i^n (\psi_{T,i} I_i + \psi_{T,i} A_i y_i^2)$$

$$I_T = \sum_i^n (\psi_{T,i} I_i + \psi_{T,i} A_i y_i^2) \quad (21)$$

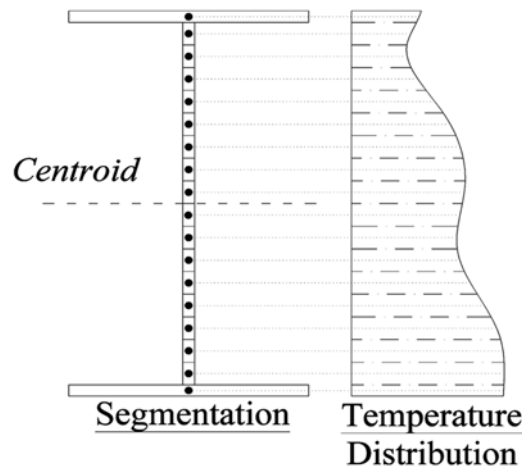


Fig. 3 Segmentation of the section under arbitrary temperature distribution

in which  $T$  is temperature level.  $\psi_T$  is the reduction factor due to material degradation of both yield stress  $\sigma_{20}$  and elastic modulus  $E_{20}$ .  $\sigma_{y20}$  and  $E_{20}$  are respectively the yield stress and elastic modulus at ambient condition.

Similarly, an equivalent plastic section modulus  $Z_{pT}$  can be evaluated by using the reduction factor  $\psi_T$  for effective yield stress  $\sigma_{20}$  as

$$\begin{aligned} \sigma_{y20}Z_{pT} &= \int_A \sigma_{yT}y dA = \int_A \sigma_{y20} \psi_T y dA = \sigma_{y20} \sum_i^n (\psi_{T,i} A_i y_i) \\ Z_{pT} &= \sum_i^n (\psi_{T,i} A_i y_i) \end{aligned} \quad (22)$$

where  $i$  is the segment number.  $I_i$  is the moment of inertia of  $i$ -th segment about its centroid.  $A_i$  is the cross section area of  $i$ -th segment.  $y_i$  is the distance from the center of an  $i$ -th segment to the centroid of the whole member section.

At elevated temperature, the material behaviour of steel deteriorates with drastic change from elastic to plastic domains is unlikely. An elliptic transition between elastic and plastic domains is assumed in the steel material at high temperature. The elliptical transition in a more pronounced nonlinear response of the structure increases with rising temperature. The effective yield stress at elevated temperature is therefore used to replace the ambient yield stress. With the effective yield stress, the strength of material still increases gradually as the residual strength. As for such nonlinear material behaviour, a set of secant elastic modulus at the corresponding temperature levels according to the  $E_T$  in Table 1 is proposed to replace the  $E$  of flexural rigidity in the stiffness formulation from Eqs. (23) to (25), which are used in order to allow for gradual yielding process at different temperature levels. The same concept is applied to tangent stiffness formulation as Eq. (10). Note that the replaced  $E$  can be input in the input data file for structural analysis software without changing the software source code, implying that engineers can perform a structural fire design using a commercial package easily.

$$M_{1n} = \left[ \frac{E_T I_T}{L} \right]_n [c_{1n}(\theta_{1n} + \theta_{2n}) + c_{2n}(\theta_{1n} - \theta_{2n})] \quad (23)$$

$$M_{2n} = \left[ \frac{E_T I_T}{L} \right]_n [c_{1n}(\theta_{1n} + \theta_{2n}) - c_{2n}(\theta_{1n} - \theta_{2n})] \quad (24)$$

$$P = E_T A_T \left[ \frac{e}{L} + \sum_{n=y,z} (b_{1n}(\theta_{1n} + \theta_{2n})^2 + b_{2n}(\theta_{1n} - \theta_{2n})^2) \right] \quad (25)$$

## 5. Numerical verifications

The proposed nonlinear structural fire analysis is carried out using the structural analysis software NIDA 2007. To verify the present results of analysis, several steel framed structures under fire are selected for comparisons and verifications. First, the experimental results of three small-scale steel

frames under fire are studied. Secondly, the results of the compartment fire in three-storey steel frame are compared. Finally, a Cardington fire test of an eight-storey framed structure is used for verification.

### 5.1 Small-scale steel frame tests under uniform heating

Three small-scale steel frames with dimensions and loading conditions as depicted on Fig. 4 are heated uniformly in a series of tests performed by Rubert and Schaumann (1986). Also the numerical results of these small-scale frames from Iu and Chan (2004) are compared. There are a series of geometry for these steel frames, which are the inverted L-sharp frame (EHR), the single-bay portal frame (EGR) and the double-bay portal frame (ZSR). These frames are also composed of the same IPE80 I-section. The material yield stress at different temperature is shown in Table 1. The frames are also effectively restrained against out-of-plane deflection. The notations of measured deformations of the small-scale steel frames are also plotted on Fig. 4.

Fig. 5 shows the deformations  $u_2$  and  $w_4$  of the EHR frame indicated in Fig. 4. The deformations from the present structural fire approach are consistent with the results from the fire tests Rubert and Schaumann (1986) and numerical results Iu and Chan (2004) in general. After  $400^\circ\text{C}$ , the significant nonlinear deformations occur, although the present fire approach can only predict the corresponding

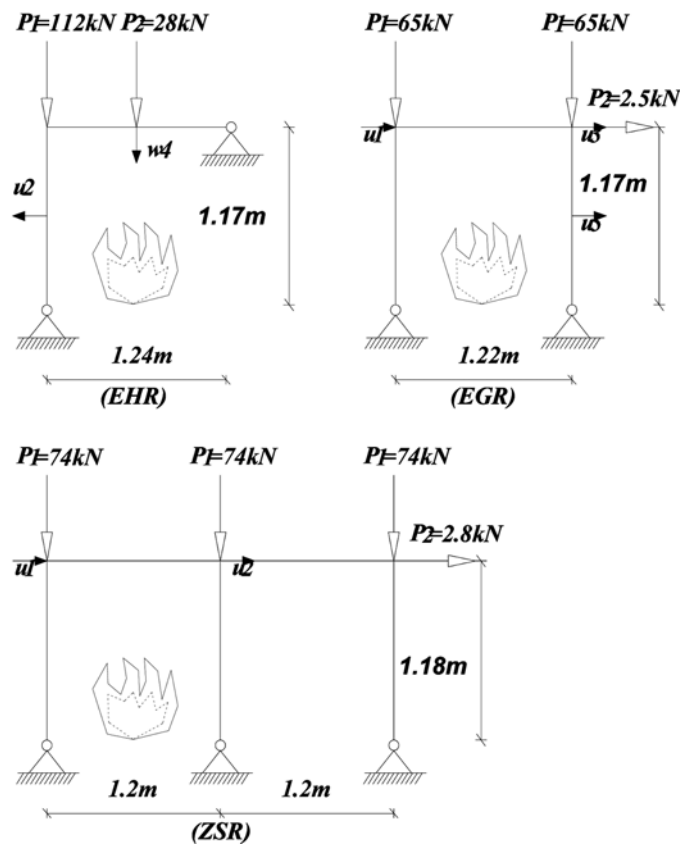


Fig. 4 Geometries and loading applications of the small-scale steel frames

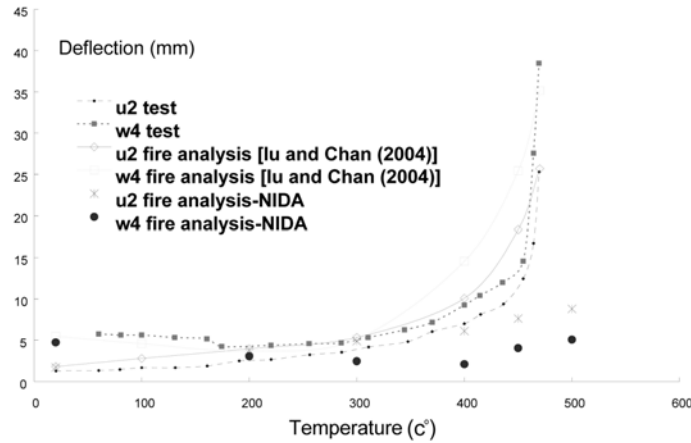


Fig. 5 Temperature-deformation curves of the EHR frame

deformations with modest magnitude because, when the displacement is large, the curve in Fig. 5 involves much nonlinearity characterized by the steep load-displacement curve in the figure that small force difference results in a large discrepancy in displacement. In respect of  $w_4$  in EHR, the mid-span deflection of beam decreases due to thermal expansion of column before  $300^{\circ}\text{C}$ . After  $300^{\circ}\text{C}$ , the deflection  $w_4$  increases considerably, as the material yielding constitutes a larger deflection component than those by thermal expansion from heated column. The deformations  $u_2$  and  $w_4$  from the present fire approach are less than those from fire test Rubert and Schaumann (1986) and numerical results Iu and Chan 2004. It is principally due to the use of elastic modulus  $E_T$  as the secant elasticity at particular temperature may not rigorously predict the gradual plasticity.

The corresponding displacements of the frames EGR and ZSR with rising temperature are also plotted in Figs. 6 and 7, respectively. These figures show that the displacements between the present analysis and both results Rubert and Schaumann (1986) and Iu *et al.* (2007) are in a good agreement until

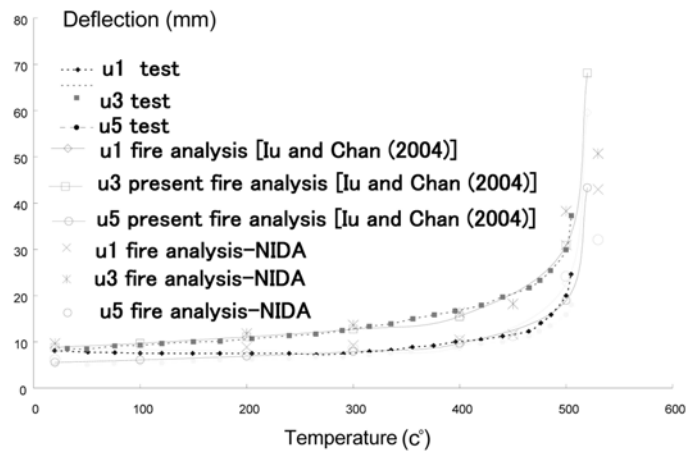


Fig. 6 Temperature-deformation curves of the EGR frame

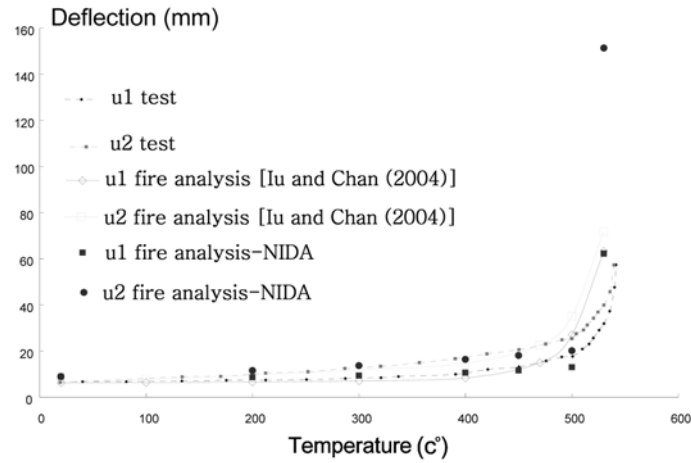


Fig. 7 Temperature-deformation curves of the ZSR frame

divergence. However, for ZSR frame,  $u_2$  from present fire approach is much greater than those from experiment by Rubert and Schaumann (1986) and from numerical results by Iu and Chan (2004). It may be mainly due to the solution being too close to the divergent point at temperature level  $530^{\circ}\text{C}$ .

### 5.2 Three-storey steel frame subject to compartment fire

Bailey (1998) numerically studied the behaviour of heated steel members in a three-storey steel frame shown in Fig. 8. A compartment fire is confined to bay 5 on the first floor in which the steel members are uniformly heated as indicated in Fig. 8. Properties and configuration of this frame and the applied loads of this numerical example are also shown in Fig. 8. All members are rigidly connected, and also the support conditions are fixed. In this verification, all members are modeled by the one element per member. The numerical results from Iu *et al.* (2007) are used for comparison.

It should be noted that the structural response predicted from the present fire analysis is stiffer than the results by Bailey 1998, but in agreement with the results by Iu *et al.* (2005). According to the numerical results from present fire analysis as shown in Fig. 9, the material of the beam commences to yield gradually after  $500^{\circ}\text{C}$ . There is a considerable nonlinear deflection between  $600^{\circ}\text{C}$  and  $606^{\circ}\text{C}$ , as the

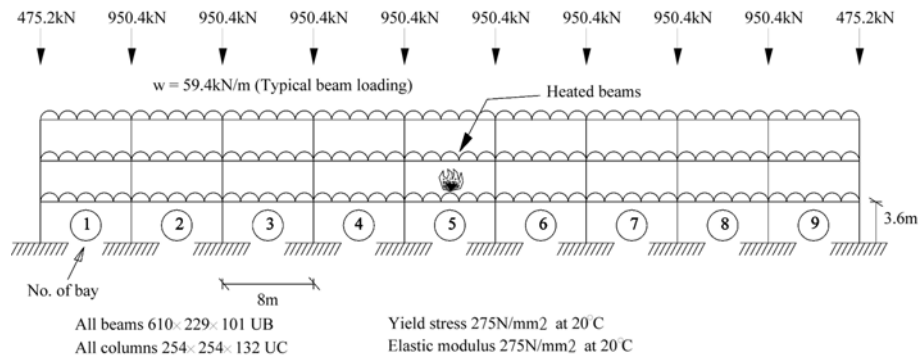


Fig. 8 Geometric configuration and material properties of a three-storey steel frame

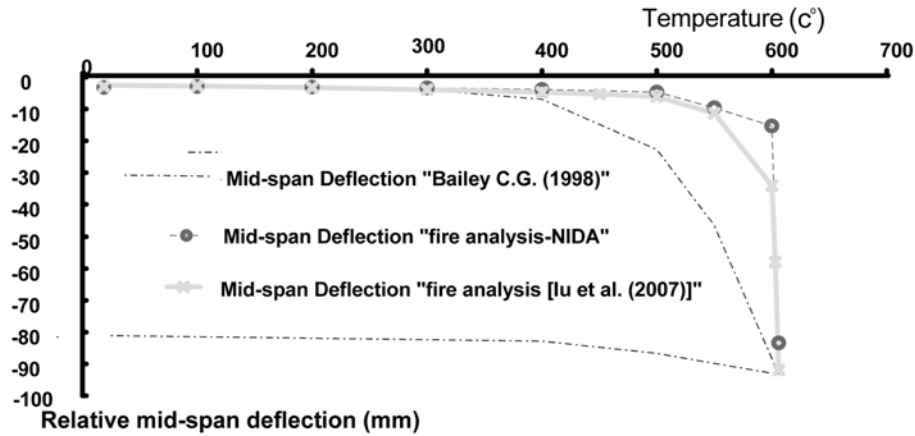


Fig. 9 Mid-span deflection of beam at bay 5 subjected to compartment fire

elastic modulus  $E_T$  is reduced nearly by half at  $600^\circ\text{C}$  at which the steel material behaves more flexibly. The maximum mid-span deflection of heated steel beam is 85 mm. As for the numerical results by Huang *et al.* (2000), the heated beam yields at the lower temperature of about  $400^\circ\text{C}$  and deflects gradually.

### 5.3 Eight-storey plane frame at Cardington fire test

The eight-storey steel frame with concrete slab was constructed as a 3 bay deep and 5 bay wide structure at the Cardington fire test in UK where four fire tests were carried out. The geometry and member section of the tested plane frame are also shown in Fig. 10. All the out-of-plane degrees of

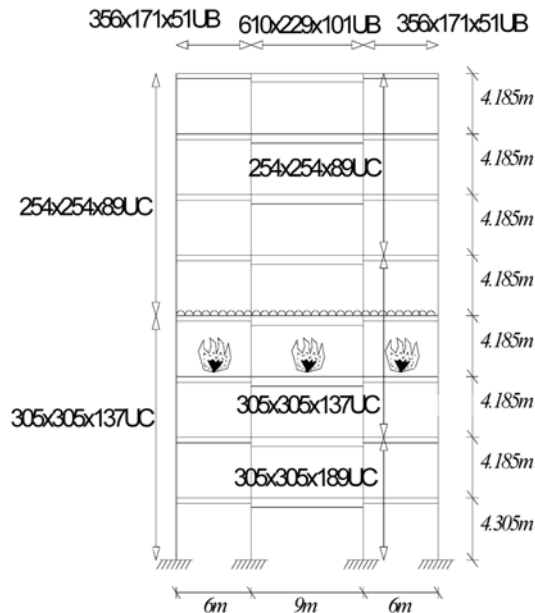


Fig. 10 Geometry and member sections of eight-storey plane frame at Cardington fire test

freedom of this frame are restrained and all connections are designed as rigid in the model for the present study. A distributed load of  $5.48 \text{ kN/m}^2$  was applied and fire was located at fourth floor. The maximum temperature is approximately  $800^\circ\text{C}$ . Although the temperature distribution across the beam at fourth floor level in the fire test is slightly non-uniform, the beam members are assumed to have been uniformly heated in the present computer modeling. The temperature distribution in the frame was described in details by many researchers, who include Plank *et al.* (1996), Kirby (1996,1997) and Sanad *et al.* (2000).

Kirby (1997) observed from the fire test that the inner primary beam deflected 293 mm at  $800^\circ\text{C}$ . Also Iu *et al.* (2005) presented the numerical results of this eight-storey plane framed structure as a comparison in this fire study with a good correlation. The beam section in Iu *et al.* (2005) is based on transformed composite section, whereas the present fire study evaluates the deflection-temperature curve of unprotected steel frame as plotted in Fig. 11. Hence there is a discrepancy between the present analysis and the results by Iu *et al.* (2005) at normal and elevated temperature before the large deflection (see Fig. 11). According to the present numerical results, the heated beam begins to yield at  $600^\circ\text{C}$  gradually and behaves nonlinearly. The mid-span deflection of a beam of  $610 \times 229 \times 101$  UB reaches 240 mm ultimately, which is close to the results from the experimental results by Kirby (1997) and Sanad *et al.* (2000).

## 6. Conclusions

The present structural fire study indicates that the nonlinear fire analysis by means of a second-order structural analysis software like NIDA can be efficiently carried out for the framed structures. In spite of its simplicity, the present fire study indicates that the structural behaviour of the framed structure under fire is generally in good agreement with different numerical and experimental results. Using the proposed method, the present simulation-based fire analysis can assist to understand the overall structural behaviour of complicated and large steel structures under fires. In addition, when the fire assessment of a framed structure is considered as a whole, fire protection of many elements in a steel building structure was found to be unnecessary in many cases because of the beneficial nonlinear effects such as centenary action in deformed beams. From the results reported here, the simulation-based fire analysis carries a high potential for effective and economical design.

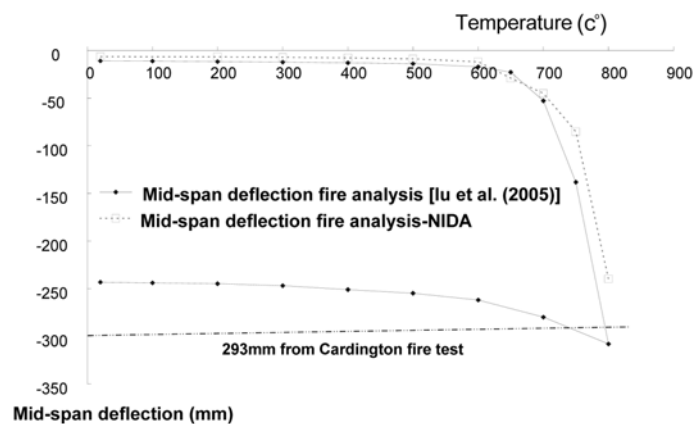


Fig. 11 Mid-span deflection of 8-storey plane frame at Cardington fire test

An integrating fire system analysis and structural design can provide an improved understanding of the real behaviour of an entire structure attacked by fire. On the other hand, the prescriptive fire design codes, which only provide the design specifications for an isolated and individual member for its limit states behaviour, are approximate and over-conservative. From this observation, the present simulation-based fire approach is suitable to the performance-based fire safety design of an overall structural system. With the advance in computer speed, availability of personal computers and structural analysis software, there will be an increasing demand for simplified, robust and efficient nonlinear analysis methods for performance-based fire safety design of structures.

## Acknowledgements

The support by the Research Grants Council (RGC) of the Hong Kong SAR Government for the project "Advanced Analysis for Progressive Collapse and Robustness Design of Steel Structures (PolyU 5115/07E)" is gratefully acknowledged.

## References

- ARBED - Research, Luxembourg/ Department of Bridge and Structural Engineering, University of Liege, Belgium - REFAO/CAFIR, computer assisted analysis of the fire resistance of steel and composite steel-concrete structures. CEC research 7210-SA/ 502, Technical reports 1 to 6, 1982/85.
- ARBED - Research, Luxembourg, University of Liege, Belgium, Buckling curves in case of fire. CEC research 7210-SA/515/931/316/618, 1992/95.
- BS5950 Part 8 (1990), Structural use of steelwork in building: Code of practice for fire resistant design.
- Bailey, C.G. (1998), "Development of computer software to simulate the structural behaviour of steel-framed building in fire", *Comput. Struct.*, **67**(6), 421-438.
- Chan, S.L. (1988), "Geometric and material nonlinear analysis of beam-columns and frames using minimum residual displacement method", *Int. J. Numer. Meth. Eng.*, **26**(12), 2657-2669.
- Chan, S.L. and Zhou, Z.H. (1995), "Second order elastic analysis of frames using single imperfect element per member", *J. Struct. Eng.-ASCE*, **121**(6), 939-945.
- Crisfield, M.A. (1981), "A faster incremental-iterative solution procedure that handles snap-through", *Comput. Struct.*, **13**(1-3), 55-62.
- Dotreppe, J.C., Franssen, J.M. and Schleich, J.B. (1982), *Computer aided fire resistance for steel and composite structures*, Review acier/Stahl/Steel No. 3.
- El-Zanaty, M.H. and Murray, D.W. (1983), "Nonlinear finite element analysis of steel frames", *J. Struct.*, **109**(2), 353-368.
- Eurocode 3. (1993), *Design of steel structures*, Pt. 1.2: structural fire design(draft). European Committee for Standardization.
- Franssen, J.M. (1987), *Etude du comportement au feu des structures mixtes acier-beton (CEFICOSS). A study of the behaviour of composite steel-concrete structures in fire*, These de Doctorat Belgique University de Liege.
- Franssen, J.M. (1990), "The unloading of building materials submitted to fire", *Fire. Safety. J.*, **16**(3), 213-237.
- Franssen, J.M., Kodur, V.K.R. and Mason, J. (2000), *User's manual for SAFIR: a computer program for analysis of structures submitted to fire*. Internal Report SPEC/2000\_03, Belgium, University of Liege, Ponts et Charpentes.
- Huang, Z., Burgess, I.W. and Plank, R.J. (1999), "Nonlinear analysis of reinforced concrete slabs subjected to fire", *ACI Struct. J.*, **96**(1), 127-135.
- Huang, Z., Burgess, I.W. and Plank, R.J. (2000), "Three-dimensional analysis of composite steel-framed buildings in fire", *J. Struct. Eng. -ASCE*, **126**(3), 389-397.

- ISO 834(1985): *Fire resistance test - elements of building construction*, International Standards Organization.
- Iu, C.K. and Chan, S.L. (2004), "A simulation-based large deflection and inelastic analysis of steel frames under fire", *J. Constr. Steel Res.*, **60**(10), 1495-1524.
- Iu, C.K., Chan, S.L. and Zha, X.X. (2005), "Nonlinear pre-fire and post-fire analysis of steel frames", *Eng. Struct.*, **27**(11), 1689-1702.
- Iu, C.K., Chan, S.L. and Zha, X.X. (2007), "Material yielding by both axial and bending spring stiffness at elevated temperature", *J. Constr. Steel Res.*, **63**(5), 677-685.
- Jeanes, D.C. (1982), *Predicting fire endurance of steel structures*, Preprint 82-033, ASCE Convention, Nevada, April 26-30, ASCE.
- Jeanes, D.C. (1985), "Applications of the computer in modeling the endurance of structural steel floor systems", *Fire. Safety. J.*, **9**(1), 119-135.
- Kirby, B.R. (1996), "British steel technical European fire test programme: design, construction and results", *Proceedings of the 2<sup>nd</sup> Cardington conference: Fire, static and dynamic tests of building structure*, **2**, 111-126.
- Kirby, B.R. (1997), "Large-scale fire tests: the British steel European collaborative research programme on the BRE 8-storey frame", *Fire safety science: Proceedings of the fifth international symposium*, **5**, 1129-1140.
- Landesmann, A., Batista, E.M. and Drummond Alves, J.L. (2005), "Implementation of advanced analysis method for steel-framed structures under fire conditions", *Fire. Safety. J.*, **40**(4), 339-366.
- Liew, J.Y.R., Tang, L.K., Holmaas, T. and Choo, Y.S. (1998), "Advanced analysis for the assessment of steel frames in fire", *J. Constr. Steel Res.*, **47**(1), 19-45.
- Liew, J.Y.R. (2004), "Performance based fire safety design of structures - A multi-dimensional integration", *Adv. Struct. Eng.*, Multi-Science, **7**(4), 111-133.
- Lim, L., Buchanan, A., Moss, P. and Franssen, J.M. (2004a), "Computer modeling of restrained reinforced concrete slabs in fire conditions", *J. Struct. Eng.*, **130**(12), 1964-1971.
- Lim, L., Buchanan, A., Moss, P. and Franssen, J.M. (2004b), "Numerical modeling of two-way reinforced concrete slabs in fire", *Eng. Struct.*, **26**(8), 1081-1091.
- Ma, K.Y. and Liew, J.Y.R. (2004), "Nonlinear plastic hinge analysis of three-dimensional steel frames in fire", *J. Struct. Eng.* -ASCE, **130**(7), 981-990.
- Najjar, S.R. and Burgess, I.W. (1996), "A nonlinear analysis for three-dimensional steel frames in fire conditions", *Eng. Struct.*, **18**(1), 77-89.
- NIDA (2007), *Non-linear integrated design and analysis (NAF-NIDA)*, version 7.
- Schleich, J.B., Dotreppe, J.C. and Franssen, J.M. (1986), "Numerical simulations of fire resistance tests on steel and composite structural elements or frames", *Fire Safety Science: Proceedings of the First International Symposium*, 311-323.
- Plank, R.J., Burgess, I.W. and Bailey, C.G. (1996), "Modeling the behaviour of steel-framed building structures by computer", *Proceedings of the 2<sup>nd</sup> Cardington conference: Fire, static and dynamic tests of building structures*, **2**, 145-160.
- Rubert, A. and Schaumann, P. (1986), "Structural steel and plane frame assemblies under fire action", *Fire. Safety. J.*, **10**(3), 173-184.
- Saab, H.A. and Nethercot, D.A. (1991), "Modelling steel frame behaviour under fire conditions", *Eng. Struct.*, **13**(4), 371-382.
- Sanad, A.M., Rotter, J.M., Usmani, A.S. and O'Connor, M.A. (2000), "Composite beams in large buildings under fire: numerical modeling and structural behaviour", *Fire Safety. J.*, **35**(3), 165-188.
- Vila Real, P.M.M., Lopes, N., Simoes da Silva, L., Piloto, P. and Franssen, J.M. (2004), "Numerical modeling of steel beam-columns in case of fire-comparisons with Eurocode3", *Fire Safety. J.*, **39**(1), 23-39.